Asian Pacific Journal of Tropical Biomedicine

Journal homepage: www.apjtb.org

doi: 10.4103/2221-1691.242291

Identification of commonly regulated protein targets and molecular pathways in PC-3 and DU145 androgen-independent human prostate cancer cells treated with the curcumin analogue 1,5-bis(2-hydroxyphenyl)-1,4-pentadiene-3-one

Kamini Citalingam[1], Faridah Abas[2,3*], Nordin H. Lajis[2*], Iekhsan Othman[1*], Rakesh Naidu[1*✉]

[1]*Jeffery Cheah School of Medicine and Health Sciences, Monash University Malaysia, Jalan Lagoon Selatan, 47500 Bandar Sunway, Selangor, Malaysia*

[2]*Laboratory of Natural Products, Faculty of Science, Universiti Putra Malaysia, 43400 UPM Serdang, Selangor, Malaysia*

[3]*Department of Food Science, Faculty of Food Science and Technology, Universiti Putra Malaysia, 43400 UPM Serdang, Selangor, Malaysia*

ARTICLE INFO

Article history:
Received 10 July 2018
Revision 2 August 2018
Accepted 10 September 2018
Available online 27 September 2018

Keywords:
Androgen-independent prostate cancer
Diarylpentanoid
Proteomics profiling
Mass spectrometry
Pathway analysis

ABSTRACT

Objective: To identify mutually regulated proteins in PC-3 and DU145 androgen-independent prostate cancer cell lines treated with 1,5-bis(2-hydroxyphenyl)-1,4-pentadiene-3-one (MS17), and to study the molecular pathways that contributed to the anticancer activity of MS17. **Methods:** PC-3 and DU145 cells were treated with 3 × EC_{50} (15 μM) concentration of MS17 for 24 h and were subjected to protein expression profiling using two-dimensional gel electrophoresis and protein identification by mass spectrometry. Selected differentially expressed proteins with significant *P*-value of $P<0.05$ and fold change over 1.5-folds were filtered through and ontologically classified. Mutually regulated proteins were ranked by fold change and identified as common protein targets of MS17. **Results:** Profiling data revealed that, the mutually down-regulated proteins included ACTB and ACTG associated with structural molecule activity, ACTN1 with cell cycle, ACTN4 with cell migration, HNRPK with apoptosis, PLST with morphogenesis and TERA with proteolysis. However, the expressions of CH60 and HS71A respectively associated with response to unfolded protein demonstrated opposing regulation in PC-3 and DU145 cells. Pathway analysis of the differentially expressed proteins in PC-3 cells demonstrated the modulation of top pathways associated with cell-cell adhesion and cytoskeletal organization while in DU145 cells the pathways were associated with proteosomal degradation, regulation of electrolytes and water, regulation control of germ cells and organization of filament assembly/disassembly. **Conclusions:** The findings of the present study provide an understanding on the anti-tumorigenic activity of MS17 at the proteome level and warrant further research for its potential application for the management and treatment of androgen-independent prostate cancer.

✉Corresponding author: Rakesh Naidu, Jeffery Cheah School of Medicine and Health Sciences, Monash University Malaysia, Jalan Lagoon Selatan, 47500 Bandar Sunway, Selangor, Malaysia.
E-mail: kdrakeshna@hotmail.com

Foundation project: This study was financially supported by the Fundamental Research Grant Scheme, (FRGS/1/2016/SKK08/MUSM/02/1) under the Ministry of Higher Education, Malaysia.

*These authors contributed equally to this work.

How to cite this article: Citalingam K, Abas F, Lajis NH, Othman I, Naidu R. Identification of commonly regulated protein targets and molecular pathways in PC-3 and DU145 androgen-independent human prostate cancer cells treated with the curcumin analogue 1,5-bis(2-hydroxyphenyl)-1,4-pentadiene-3-one. Asian Pac J Trop Biomed 2018; 8(9): 436-445.

1. Introduction

The study of proteomics using 2-dimensional gel electrophoresis (2-DE) and mass spectrometry for protein identification has become a powerful tool for the comprehensive analysis of specific protein target along with their interacting partners and networks in order to understand cellular processes. As proteins are the key players that have regulatory roles to influence cell growth in tumorigenesis, proteins may regulate cellular response towards drug treatment. Proteomics study is therefore required to understand the potential regulatory mechanism of a candidate anticancer agent in elucidating its involvement in cancer progression and in the hope of identifying target proteins in response to treatment for therapeutic management of prostate cancer.

Curcumin is the most studied phytochemical extracted from the plant *Curcuma longa*. Curcumin significantly inhibits prostate cancer cell growth and prevents the progression of the tumour to its hormone-refractory stage by interfering with the signalling pathways in androgen-dependent and -independent prostate cancer cells[1,2]. While phase Ⅰ clinical trials have already proven the safety profile of curcumin even at high doses, the clinical application of this compound remains limited due to its poor pharmacokinetic properties. Analogues of curcumin such as diarylpentanoids, a group of curcumin-like analogues with 5-carbon chain between its aryl rings that demonstrated to be effective at lower concentration and improved growth suppressive activity have been developed in recent years[3]. Diarylpentanoid EF24 [3,5-bis(2-fluorobenzylidene)-4-piperidone] was reported to demonstrate potent anti-tumorigenic effects on cancer cells compared to curcumin[4]. Similarly, other studies on diarylpentanoids ca27 and Ca 37 which are structurally identical to MS17 [1, 5-bis(2-hydroxyphenyl)-1,4-pentadiene-3-one] were reported to exhibit anticancer activity on prostate cancer cells[5,6]. However, the molecular mechanisms that demonstrate its anticancer activity were not determined in prostate cancer cells. In our previous findings, MS17 showed growth inhibition, cytotoxicity and cell death inducing activities on androgen-nonresponsive prostate cancer (PC-3 and DU145) and cervical cancer (HeLa and CaSki) cells[7,8]. MS17 demonstrated significant apoptotic activity at 24 h following treatment with 3 × EC_{50} (15 μM) concentration in PC-3 and DU145 cells[7]. MS17 demonstrated potent cytotoxicity effect on cancer cells with lower toxicity against normal cells compared to curcumin. Therefore, the focus of the current study is to perform protein expression profiling on treated PC-3 and DU145 cells to identify mutually regulated proteins as common targets in both of these cell lines as well as molecular pathways that contribute to the anticancer activity of MS17 using 2-DE and nanoflow liquid choromatography electrospray-ionisation coupled with mass spectrometry/mass spectrometry (LC-MS/MS).

2. Materials and methods

2.1. Cell culture and MS17 diarylpentanoid

The human androgen-independent metastatic prostate cancer cell lines, PC-3 and DU145 were purchased from American Type Culture Collection (ATCC, Rockville, USA) and maintained using appropriate media under standard conditions as previously described[7]. The chemically purified diarylpentanoid, MS17 was synthesized and prepared based on the method described previously[9].

2.2. Treatment and total protein extraction

Cells were plated in a 75 cm^2 tissue culture flasks, treated with 15 μM dose of MS17 and incubated in a humidified incubator for 24 h. All treatments were performed in triplicates and fresh medium containing 0.5% DMSO was added to the untreated control cells. Following incubation, cells were harvested and washed with ice cold PBS solution twice before protein lysate was extracted from the treated and untreated cells. Cell pellets were resuspended in 1 mL lysis buffer containing 7 M urea, 2 M thiourea, 4% CHAPS, 65 mM dithiothreitol (DTT), 2% immobilized pH gradient (IPG) buffer and protease inhibitor mix. Suspensions were vortexed on ice at 2 500 rpm for 2 min and frozen on dry ice for 10 min. The second cycle of freeze-thaw was performed for 5 min. Then, the samples were vortexed on ice at 2 500 rpm for another 15 min. DNase Ⅰ (Qiagen, Valencia, CA., USA) and RNase A (Thermo Scientific, USA) at final concentrations of 20 units/mL and 0.25 mg/mL respectively were added into each sample to eliminate any DNA contaminants and subsequently incubated on ice for another 45 min. Following incubation, the protein lysate was centrifuged at 13 000 × *g* at 4 ℃ for 1 h and the supernatants of the treated and untreated samples were collected in sterile microcentrifuge tubes and placed on ice before protein concentration was quantified with the 2D Quant kit (GE Healthcare, UK) based on the protocol provided by the manufacturer.

2.3. 2-DE

Appropriate amount of individual protein samples was adjusted with the addition of rehydration buffer [7 M urea, 2 M thiourea, 2% (w/v) CHAPS, 65mM DTT, 0.2% Triton X-100, 1% bromophenol blue, 0.5% (v/v) IPG buffer] to a final concentration of 1 mg and incubated for 30 min at room temperature. The protein samples were then applied to IPG strips (13 cm, pH 3-10 linear) on Immobiline DryStrip reswelling tray (GE Healthcare, Buckinghamshire, UK) and allowed to rehydrate for 18 h at room temperature. Following rehydration, isoelectric focusing was performed at 20 ℃ in a stepwise voltage ramp using Ettan IPGphorⅢ system (GE Healthcare, UK): 500 V for 2 h 20 min, hold; 1 000 V for 1 h, gradient; 8 000 V for 2 h 30 min, gradient, and 8 000 V for 30 min, hold. Once isoelectric focusing was completed, the IPG strips were equilibrated in equilibration buffer [375 mM Tris-HCL (pH 8.8), 6 M urea, 30% (v/v) glycerol, 2% (w/v) SDS, 0.002% bromophenol blue and 1% (w/v) DTT] for 30 min, followed by the same buffer containing 2.5% (w/v) iodoacetamide instead of DTT for another 30 min. The second dimensional SDS-PAGE was carried out on 12% SDS-polyacrylamide gels at 18 ℃ in Laemmli running buffer using a Hoefer SE600 system (GE Healthcare, UK). Separation was performed at 90 V for 30 min and 200 V constant power till the bromophenol dye front reached the bottom of the gels. Upon completion, the gels were fixed in 10% methanol, stained in

Coomassie brilliant blue G-250, destained in a mixture of 50% ethanol and 12% acetic acid until the background was clear. The experiment was performed in three biological replicates.

2.4. Protein visualization and image analysis

Gel images were scanned using a ChemiDoc™ XRS Imaging System (Bio-Rad, USA) and captured using Quantity One® Software (Bio-Rad,USA). Spot detection and matching between gels were automatically performed using the PDQuest software version 8.0.1 (Bio-Rad, USA). The PDQuest software was also used to assign identification number and to calculate intensity of each protein spot. Selected spots were filtered based on sensitivity value of 25.0, minimal peak value of 1 000 with Gaussian modelling. Each spot volume from replicate gel was normalized relative to the total spot volume of the control gel. Relative comparison of the spot intensity abundance between treated and untreated control groups was analyzed with Student's *t*-test. Statistical significance was set as $P<0.05$ and significant protein spots with at least 1.5-fold differences were selected for protein identification.

2.5. In-gel tryptic digestion

Protein spots of interest from the treated and control gels were excised manually and transferred to 0.5 mL microfuge tubes for tryptic digestion. The pooled gel pieces were incubated several times with 200 μL of 200 mM ammonium bicarbonate in 40% acetonitrile (ACN) for 30 min at 37 ℃ to remove excess dye. The solvent was discarded and 20 μL of trypsin solution was then added to the gel plugs and subsequently incubated for 5 min at room temperature. Next, 50 μL of digestion buffer (40 mM ammonium bicarbonate in 9% ACN) were added to the gel plugs and left incubated overnight at 37 ℃. After overnight incubation, the supernatants were collected and saved into separate collection tubes. The gel pieces were then extracted with 50 μL of 5% formic acid followed by a mixture of 5% formic acid / 50% ACN and lastly with 50 μL HPLC grade pure ACN with 15 minutes incubation in between solutions at 37 ℃. Supernatant was collected and the gel pieces were discarded. The pooled extracts were then dried overnight at 60 ℃ using centrifugal evaporator CVE-3100 (Eyela, Japan).

2.6. LC-MS/MS analysis

The dried peptides were reconstituted with 8 μL of 0.1% formic acid in water and loaded into Agilent C18 300A Large Capacity Chip (Agilent Technologies, USA) and equilibrated with 0.1% formic acid in water. The following gradient: 5%-75% formic acid in water from 0-30 min followed by 75%-75% formic acid in water from 30-39 min was used to elute the peptides from the column. Q-TOF polarity was set at positive with capillary and fragmentor voltage being set at 1 790 V and 175 V respectively and 5 L/min of gas flow at 325 ℃. Protein spectra were analyzed in auto MS mode ranging from 110-3 000 *m/z* for MS scan and 50-3 000 *m/z* for LC-MS/MS scan. Data obtained from LC-MS/MS was processed with PEAKS Studio 7.0 software (Bioinformatics Solution, Waterloo, Canada).

2.7. Protein identification and data analysis

Protein identification by automated *de nova* sequencing was determined using PEAKS studio 7.0 software. Protein homology of each sample was searched against *Homo sapiens* protein database in the UniProtKB/Swiss-Prot database (December 2015) by comparing the *de nova* sequence tag. Parent mass and fragment mass error tolerance were set at 0.1Da with monoisotopic as precursor mass search type. Carbamidomethylation was set as fixed modification and maximum mixed cleavages at 3. Trypsin was used for protein digestion. The search results were filtered based on the following criteria to minimize false positive results: i) False Discovery rate (FDR) < 1.0% and ii) PEAK Score (-logP) > 20. Peptides that did not satisfy the set parameters were excluded from analysis. LC-MS/MS spectra were also searched against cRAP protein database in The Global Proteome Machine (Version 2012.01.01) to eliminate possible common contaminants. The list of proteins that satisfy the above criteria was considered as differentially expressed proteins (DEPs). In addition, DEPs with a protein score (-10logP) cut-off > 50 and identified with at least two peptides, which imposed a percentage coverage of > 15% and fold change values > 1.0-fold were considered for further analysis.

2.8. Bioinformatics analysis

The lists of DEPs were analysed based on gene ontology classification using PANTHER™ classification system (http://pantherdb.org/) to classify them according to their biological processes/molecular function. Accession numbers of the DEPs were imported into Ingenuity® Pathway Analysis (IPA) software (IPA®; QIAGEN Redwood City) for identification of top significant canonical pathways. Using right-tailed Fisher Exact test *P*-value set at $P<0.05$, canonical pathways were considered as statistically significant when it passed through a threshold of 1.3 [calculated by –log (*P*-value)]. In addition, the DEPs within the top five identified pathways were extracted and overlaid to view their protein interaction network using the MyPathway design tool.

3. Results

3.1. Protein expression profiling and gene ontology classification analysis

PC-3 and DU145 cells were treated with 3 × EC_{50} (15 μM) dose of MS17 and DMSO (control) respectively for 24 h. Using the PDQuest software, protein spots with significant *P*-value of $P<0.05$ and a fold change over 1.5-fold in MS17 treated cells compared to control cells in replicate gels were averaged and quantified. Overall, a total of 20 significant protein spots were detected in PC-3 cells while 24 spots were detected in DU145 cells, as indicated by the specific spot number (SSP number). Representative 2-DE gel images of control and MS17-treated cells in PC-3 and DU145 cells are respectively shown in Figures 1 and 2. Protein identification by PEAKS software and UniProt/SwissProt database identified a total of 46 DEPs in PC-3 cells and 47 DEPs in DU145 cells. Amongst these DEPs, a

total of 10 up- and 36 down-regulated (Table 1) were obtained in PC-3 cells while 24 up- and 23 down-regulated (Table 2) DEPs were selected in DU145 cells. The significant regulated proteins were then ontologically classified based on their biological processes or molecular functions.

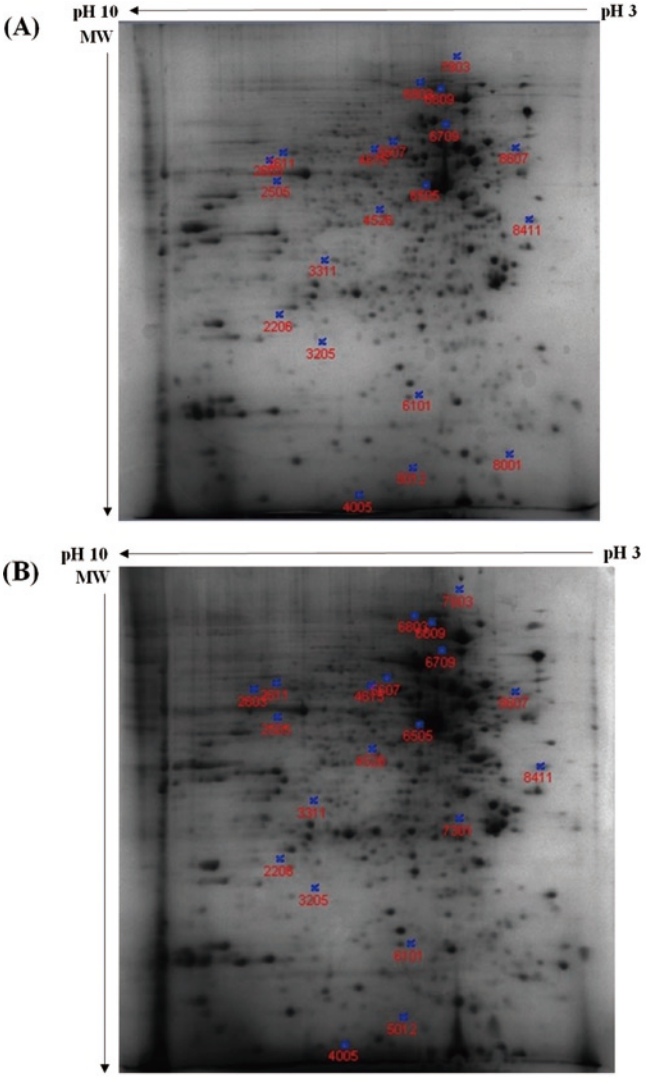

Figure 1. Representative 2-DE gel images of protein expression in (A) control and (B) 15 μM-treated PC-3 cells.
Selected proteins correlating with the specific spot number (SSP) were listed in Table 1.

Based on the PANTHER classification analysis, a total of 12 functional categories were identified in PC-3 and 11 in DU145 cells. Among these categories in PC-3 cells, metabolic process constitutes for the major proportion (23%) followed by apoptosis and cell cycle each comprised of 13%, protein folding 9% while proteolysis, regulation of transcription, structural molecule activity and transporter activity account for 7% respectively. However, the other functional categories including cell migration, morphogenesis and response to unfolded protein constitute 12%, each with 4% and cell adhesion accounts for 2% of the DEPs. Similarly, among the 11 functional categories associated with DU145 cells, the largest category was metabolic process (20%) followed by response to unfolded protein (17%). Apoptosis, cytoskeletal organization and proteolysis account for approximately 11% respectively while regulation of transcription, structural molecule activity and transporter activity account for 6% respectively. However, the other functional categories including cell migration, morphogenesis and signal transduction activity represent 12% of the DEPs, each with 4%.

Amongst the total DEPs, 9 regulated proteins in PC-3 (Table 1) and DU145 (Table 2) cells were identified as mutually expressed proteins and common protein targets of MS17 in both the cell lines. The mutually down-regulated proteins included, ACTB and ACTG which were associated with structural molecule activity, ACTN1 with cell cycle, ACTN4 with cell migration, HNRPK with apoptosis, PLST with morphogenesis and TERA with proteolysis. Interestingly, the expressions of CH60 and HS71A respectively associated with response to unfolded protein demonstrated opposing regulation in both the cell lines. The expression of CH60 was up-regulated in PC-3 cells but down-regulated in DU145 cells while HS71A was down-regulated in PC-3 but up-regulated in DU145 cells. The selected proteins along with their corresponding functional categories were illustrated in Tables 1 and 2.

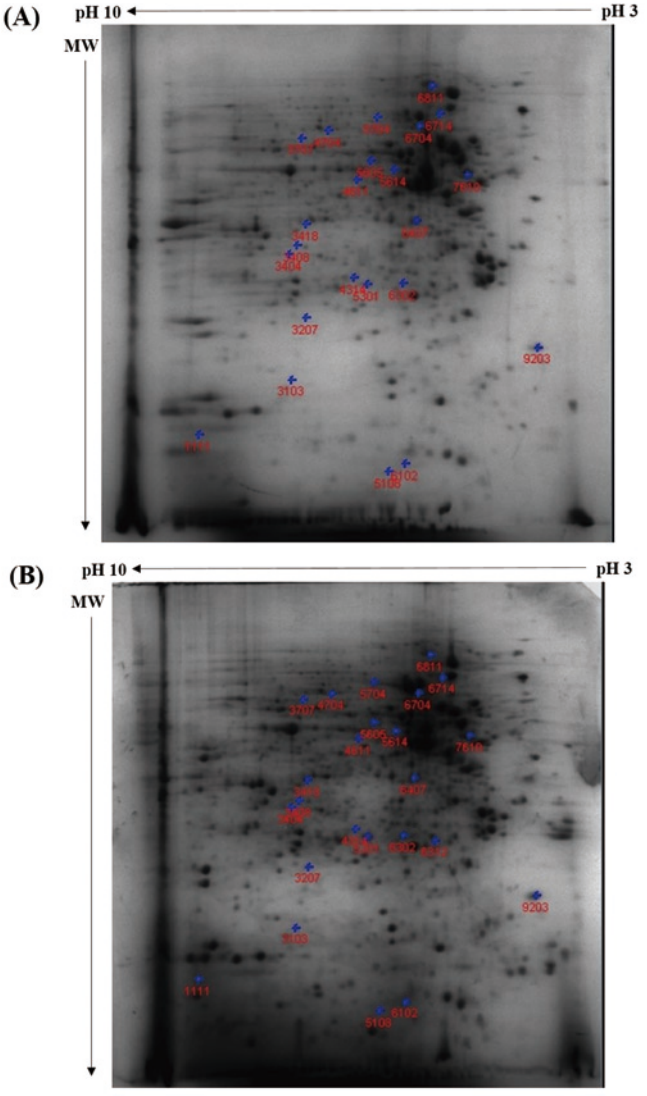

Figure 2. Representative 2-DE gel images of protein expression in (A) control and (B) 15 μM-treated DU145 cells.
Selected proteins correlating with the specific spot number (SSP) were listed in Table 2.

Table 1

Selected differentially expressed proteins (DEPs) regulated following 15 μM treatment of MS17 in PC-3 cells at 24 h.

SSP No.	Protein name	UniProt/gene symbol	Accession number	-10lgP	Coverage (%)	#Peptides/#Unique	Avg. Mass	Fold Change (15 μM)	Go Term
Up-regulated									
2603	ATP synthase subunit alpha mitochondrial	ATPA/*ATP4A1*	P25705	171.05	25	13/13	59 751	1.55	Transporter activity
2603	Glutathione reductase mitochondrial	GSHR/*GSR*	P00390	122.60	15	7/7	56 257	1.55	Transporter activity
5607	60 kDa heat shock protein mitochondrial	CH60/*HSPD1*	P10809	207.85	23	7/7	61 055	1.46	Response to unfolded protein
3311	Annexin A2	ANXA2/*ANXA2*	P07355	181.73	41	15/5	38 604	1.18	Apoptosis
3311	Beta-lactamase-like protein 2	LACB2/*LACTB2*	Q53H82	118.69	15	3/3	32 806	1.18	Metabolic process
7301	14-3-3 protein zeta/delta	1433Z/*YWHAZ*	P63104	107.54	25	6/3	27 745	1.13	Apoptosis
7301	Proteasome subunit alpha type-3	PSA3/*PSMA3*	P25788	153.57	38	8/8	28 433	1.13	Apoptosis
7301	Inositol monophosphatase 1	IMPA1/*IMPA1*	P29218	144.91	35	11/11	30 189	1.13	Metabolic process
7301	Ornithine aminotransferase mitochondrial	OAT/*OAT*	P04181	138.45	15	5/5	48 535	1.13	Metabolic process
7301	Pyridoxal kinase	PDXK/*PDXK*	O00764	93.05	19	4/4	35 102	1.13	Metabolic process
Down-regulated									
6803	Vinculin	VINC/*VCL*	P18206	361.06	42	74/74	123 799	-1.12	Cell adhesion
6803	Ubiquitin-like modifier-activating enzyme 1	UBA1/*UBA1*	P22314	175.33	17	12/12	117 849	-1.12	Proteolysis
4526	Serine/threonine-protein phosphatase PP1-alpha catalytic subunit	PP1A/*PPP1CA*	P62136	149.35	39	11/11	37 512	-1.37	Cell cycle
4526	Alpha-enolase	ENOA/*ENO1*	P06733	218.58	34	12/12	47 169	-1.37	Metabolic process
4526	Phosphoglycerate kinase 1	PGK1/*PGK1*	P00558	297.29	55	39/30	44 615	-1.37	Metabolic process
4526	Phosphoglycerate kinase 2	PGK2/*PGK2*	P07205	193.13	24	12/3	44 796	-1.37	Metabolic process
4526	Transaldolase	TALDO/*TALDO1*	P37837	139.73	24	8/8	37 540	-1.37	Metabolic process
4526	Vacuolar protein sorting-associated protein VTA1 homolog	VTA1/*VTA1*	Q9NP79	123.44	25	6/6	33 879	-1.37	Transporter activity
4005	Pterin-4-alpha-carbinolamine dehydratase	PHS/*PCBD1*	P61457	146.22	61	12/12	12 000	-1.46	Regulation of transcription
6809	Alpha-actinin-1	ACTN1/*ACTN1*	P12814	307.89	59	60/30	103 058	-1.87	Cell cycle
6809	Alpha-actinin-2	ACTN2/*ACTN2*	P35609	184.73	21	23/2	103 854	-1.87	Cell migration
6809	Alpha-actinin-4	ACTN4/*ACTN4*	O43707	268.93	51	47/20	104 854	-1.87	Cell migration
6809	Acylamino-acid-releasing enzyme	ACPH/*APEH*	P13798	158.76	18	12/12	81 225	-1.87	Proteolysis
6809	Transitional endoplasmic reticulum ATPase	TERA/*VCP*	P55072	328.77	54	43/43	89 322	-1.87	Proteolysis
6505	Creatine kinase B-type	KCRB/*CKB*	P12277	96.25	18	5/5	42 644	-1.97	Metabolic process
6505	Activator of 90 kDa heat shock protein ATPase homolog 1	AHSA1/*AHSA1*	O95433	120.27	29	6/6	38 274	-1.97	Protein folding
6505	Beta-actin-like protein 2	ACTBL/*ACTBL2*	Q562R1	145.45	23	11/5	42 003	-1.97	Structural molecule activity
6505	Actin cytoplasmic 2	ACTG/*ACTG1*	P63261	255.84	64	36/15	41 793	-1.97	Structural molecule activity
2611	Annexin A11	ANX11/*ANXA11*	P50995	269.58	37	23/23	54 390	-2.08	Apoptosis
2611	Pyruvate kinase PKM	KPYM/*PKM2*	P14618	320.58	53	30/30	57 937	-2.08	Apoptosis
2611	Tubulin alpha-1C chain	TBA1C/*TUBA1C*	Q9BQE3	115.05	24	9/4	49 895	-2.08	Cell cycle
2611	Tubulin alpha-3C/D chain	TBA3C/*TUBA3C*	Q13748	102.25	21	7/2	49 960	-2.08	Cell cycle
2611	Tubulin beta chain	TBB5/*TUBB*	P07437	102.26	20	7/7	49 671	-2.08	Cell cycle
2611	Aldehyde dehydrogenase family 1 member A3	ALIA3/ *ALDH1A3*	P47895	229.16	32	16/15	56 109	-2.08	Metabolic process
6709	Heterogeneous nuclear ribonucleoprotein K	HNRPK/ *HNRNPK*	P61978	182.09	42	18/18	50 976	-2.58	Apoptosis
6709	Plastin-2	PLSL/*LCP1*	P13796	203.78	49	33/26	70 289	-2.58	Morphogenesis
6709	Plastin-3	PLST/*PLS3*	P13797	138.03	16	11/4	70 811	-2.58	Morphogenesis
6709	78 kDa glucose-regulated protein	GRP78/*HSPA5*	P11021	176.74	38	23/23	72 333	-2.58	Protein folding
6709	Protein disulfide-isomerase A4	PDIA4/*PDIA4*	P13667	82.34	16	8/8	72 933	-2.58	Protein folding
6709	Heat shock 70 kDa protein 1A	HS71A/*HSPA1A*	P0DMV8	144.80	18	9/9	70 052	-2.58	Response to unfolded protein
6709	Actin cytoplasmic 1	ACTB/*ACTB*	P60709	137.57	27	10/10	41 737	-2.58	Structural molecule activity
4615	Tubulin beta-4B chain	TBB4B/*TUBB4B*	P68371	121.00	22	9/2	49 831	-2.71	Cell cycle
4615	Thioredoxin reductase 1 cytoplasmic	TRXR1/ *TXNRD1*	Q16881	176.21	20	8/8	70 906	-2.71	Metabolic process
4615	Protein disulfide-isomerase A3	PDIA3/*PDIA3*	P30101	190.79	39	16/16	56 782	-2.71	Protein folding
8001	Transcription elongation factor B polypeptide 1	ELOC/*TCEB1*	Q15369	211.66	66	15/15	12 473	-2.94	Regulation of transcription
8001	DNA-directed RNA polymerase Ⅱ subunit RPB7	RPB7/*POLR2G*	P62487	51.46	16	2/2	19 294	-2.94	Regulation of transcription

Table 2

Selected differentially expressed proteins (DEPs) regulated following 15 μM treatment of MS17 in DU145 cells at 24 h.

SSP No.	Protein name	UniProt/Gene symbol	Accession number	−10lgP	Coverage (%)	#Peptides/#Unique	Avg. Mass	Fold Change (15 μM)	GO Term
Up-regulated									
5704	Heat shock 70 kDa protein 1A	HS71A/*HSPA1A*	P0DMV8	300.88	48	39/11	70 052	3.16	Response to unfolded protein
5704	Heat shock 70 kDa protein 6	HSP76/*HSPA6*	P17066	349.65	65	66/44	71 028	3.16	Response to unfolded protein
5704	Sec1 family domain-containing protein 1	SCFD1/*SCFD1*	Q8WVM8	111.87	15	6/6	72 380	3.16	Transporter activity
6102	Cofilin-1	COF1/*CFL1*	P23528	293.53	48	17/14	18 502	1.96	Cytoskeletal organization
6102	Adenine phosphoribosyltransferase	APT/*APRT*	P07741	188.48	46	8/8	19 608	1.96	Metabolic process
6102	Mediator of RNA polymerase Ⅱ transcription subunit 11	MED11/*MED11*	Q9P086	69.30	50	3/3	13 129	1.96	Regulation of transcription
6102	C-Myc-binding protein	MYCBP/*MYCBP*	Q99417	143.25	59	6/6	11 967	1.96	Regulation of transcription
6714	Heat shock protein HSP 90-alpha	HS90A/*HSP90AA1*	P07900	241.77	52	58/31	84 660	1.70	Response to unfolded protein
6714	Heat shock protein HSP 90-beta	HS90B/*HSP90AB1*	P08238	231.86	50	47/16	83 264	1.70	Response to unfolded protein
6714	Sorting nexin-1	SNX1/*SNX1*	Q13596	163.89	36	21/19	59 070	1.70	Transporter activity
6714	Sorting nexin-2	SNX2/*SNX2*	O60749	127.90	28	12/10	58 471	1.70	Transporter activity
6302	NADH dehydrogenase [ubiquinone] iron-sulfur protein 3 mitochondrial	NDUS3/*NDUFS3*	O75489	214.78	42	12/12	30 242	1.45	Metabolic process
6302	Phosphoserine phosphatase	SERB/*PSPH*	P78330	96.20	16	3/3	25 008	1.45	Metabolic process
1111	Profilin-1	PROF1/*PFN1*	P07737	206.80	64	13/13	15 054	1.32	Cytoskeletal organization
5301	Enoyl-CoA hydratase mitochondrial	ECHM/*ECHS1*	P30084	303.55	77	42/42	31 387	1.25	Metabolic process
5301	Peroxiredoxin-6	PRDX6/*PRDX6*	P30041	151.14	29	6/6	25 035	1.25	Metabolic process
5301	Proteasome subunit alpha type-6	PSA6/*PSMA6*	P60900	193.79	51	15/15	27 399	1.25	Proteolysis
5301	Heat shock protein beta-1	HSPB1/*HSPB1*	P04792	324.20	89	66/66	22 783	1.25	Response to unfolded protein
6312	Annexin A1	ANXA1/*ANXA1*	P04083	276.22	58	44/43	38 714	1.07	Apoptosis
7610	Vimentin	VIME/*VIM*	P08670	407.95	88	161/136	53 652	1.07	Apoptosis
7610	Desmin	DESM/*DES*	P17661	176.93	17	18/4	53 536	1.07	Cytoskeletal organization
6312	Glutathione S-transferase Mu 3	GSTM3/*GSTM3*	P21266	74.28	16	3/3	26 560	1.07	Metabolic process
6312	Ubiquitin carboxyl-terminal hydrolase isozyme L1	UCHL1/*UCHL1*	P09936	127.86	29	6/6	24 824	1.07	Proteolysis
6312	Ran-specific GTPase-activating protein	RANG/*RANBP1*	P43487	152.43	57	12/12	23 310	1.07	Signal transduction activity
Down-regulated									
6704	Heterogeneous nuclear ribonucleoprotein K	HNRPK/*HNRNPK*	P61978	241.66	62	49/48	50 976	−1.26	Apoptosis
6704	Lamin-B2	LMNB2/*LMNB2*	Q03252	223.46	64	57/55	69 948	−1.26	Apoptosis
6704	Plastin-1	PLSI/*PLS1*	Q14651	162.98	19	13/7	70 254	−1.26	Morphogenesis
6704	Plastin-3	PLST/*PLS3*	P13797	216.27	53	34/28	70 811	−1.26	Morphogenesis
6704	Ubiquitin-60S ribosomal protein L40	RL40/*UBA52*	P62987	100.37	36	5/5	14 728	−1.26	Proteolysis
6704	Ubiquitin carboxyl-terminal hydrolase 14	UBP14/*USP14*	P54578	147.20	32	15/15	56 069	−1.26	Proteolysis
6704	Poly(U)-binding-splicing factor	PUF60/*PUF60*	Q9UHX1	166.79	38	18/18	59 876	−1.26	Regulation of transcription
6704	60 kDa heat shock protein mitochondrial	CH60/*HSPD1*	P10809	151.27	25	13/13	61 055	−1.26	Response to unfolded protein
6704	Stress-70 protein mitochondrial	GRP75/*HSPA9*	P38646	196.36	40	26/24	73 681	−1.26	Response to unfolded protein
6704	Heat shock cognate 71 kDa protein	HSP7C/*HSPA8*	P11142	188.20	41	27/22	70 898	−1.26	Response to unfolded protein
6704	Ras GTPase-activating protein-binding protein 1	G3BP1/*G3BP1*	Q13283	118.31	19	7/7	52 164	−1.26	Signal transduction activity
6704	Actin cytoplasmic 1	ACTB/*ACTB*	P60709	152.42	32	12/11	41 737	−1.26	Structural molecule activity
3418	Malate dehydrogenase cytoplasmic	MDHC/*MDH1*	P40925	229.44	43	15/15	36 426	−1.27	Metabolic process
3418	PDZ and LIM domain protein 1	PDLI1/*PDLIM1*	O00151	123.13	35	7/7	36 072	−1.27	Metabolic process
3418	39S ribosomal protein L39 mitochondrial	RM39/*MRPL39*	Q9NYK5	138.59	28	9/9	38 712	−1.27	Metabolic process
3418	LIM and SH3 domain protein 1	LASP1/*LASP1*	Q14847	108.78	18	4/4	29 717	−1.27	Structural molecule activity
6811	Alpha-actinin-1	ACTN1/*ACTN1*	P12814	258.10	51	40/17	103 058	−1.62	Cell migration
6811	Alpha-actinin-4	ACTN4/*ACTN4*	O43707	304.03	63	52/29	104 854	−1.62	Cell migration
6811	Keratin type I cytoskeletal 16	K1C16/*KRT16*	P08779	171.29	38	13/8	51 268	−1.62	Cytoskeletal organization
6811	Src substrate cortactin	SRC8/*CTTN*	Q14247	209.78	33	16/16	61 586	−1.62	Cytoskeletal organization
6811	Transitional endoplasmic reticulum ATPase	TERA/*VCP*	P55072	427.36	80	107/107	89 322	−1.62	Proteolysis
6811	Actin cytoplasmic 2	ACTG/*ACTG1*	P63261	192.24	50	14/13	41 793	−1.62	Structural molecule activity
5108	Proteasome subunit beta type-1	PSB1/*PSMB1*	P20618	236.56	32	10/10	26 489	−2.18	Apoptosis

Table 3
Top 5 canonical pathways significantly modulated by the DEPs in 15 μM-treated PC-3 and DU145 cells.

Canonical pathways	#Nominal *P*-value	Genes
PC-3		
Remodeling of epithelial adherens junctions	5.89E-08	*TUBB4B, ACTB, VCL, ACTN4, ACTG1, ACTN1*
Epithelial adherens junction signaling	2.75E-06	*TUBB4B, ACTB, VCL, ACTN4, ACTG1, ACTN1*
Sertoli cell-sertoli cell junction signaling	3.16E-06	*TUBB4B, ACTB, VCL, ACTN4, ACTG1, ACTN1*
Paxillin signaling	8.51E-06	*ACTB, VCL, ACTN4, ACTG1, ACTN1*
Germ cell-sertoli cell junction signaling	9.77E-06	*TUBB4B, ACTB, VCL, ACTN4, ACTG1, ACTN1*
DU145		
Protein ubiquitination pathway	3.39E-08	*UCHL1, HSPA8, PSMA6, USP14, HSP90AB1, HSPA9, PSMB1, HSPA1A/1B, HSP90AA1, HSPD1, HSPB1*
Aldosterone signaling in epithelial cells	1.91E-06	*HSPA8, HSP90AB1, HSPA9, HSPA1A/1B, HSP90AA1, HSPD1, HSPB1*
Germ cell-sertoli cell junction signaling	8.51E-06	*CFL1, ACTB, ACTN4, CLINT1, ACTG1, ACTN1, PLS1*
Sertoli cell-sertoli cell junction signaling	3.98E-05	*ACTB, ACTN4, CLINT1, ACTG1, ACTN1, PLS1*
Actin cytoskeleton signaling	1.41E-04	*PFN1, CFL1, ACTB, ACTN4, ACTG1, ACTN1*

Green represents down-regulated genes while red indicates up-regulated genes.

3.2. Pathway analysis

The deregulated DEPs were mapped to biological canonical pathways to identify and understand the cellular pathways that were significantly modulated by MS17 treated prostate cancer cells. The top 5 canonical pathways of PC-3 and DU145 cells that were significantly activated by treatment were selected for further analysis. For each pathway, the nominal *P*-value along with all the input proteins that are encoded by its respective genes was presented in Table 3.

In PC-3 cells, the pathways, "Remodeling of Epithelial Adherens Junctions", "Epithelial Adherens Junction Signaling", "Sertoli Cell-Sertoli Cell Junction Signaling" and "Germ Cell-Sertoli Cell Junction Signaling" were associated with the down-regulation of TUBB4B, ACTB, VCL, ACTN4, ACTG1 and ACTN1 while "Paxillin Signaling" pathway was modulated by the down-regulation of ACTB, VCL, ACTN4, ACTG1 and ACTN1 (Table 3). On the other hand, the two most significantly activated pathways in DU145 cells; "Protein Ubiquitination Pathway" and "Aldosterone Signaling in Epithelial Cells" were associated with the up-regulation of HSPA1A/HSPA1B, HSP90AA1, HSP90AB1 and HSPB1 and the repressed expression of HSPA8, HSPA9 and HSPD1. In addition, "Protein Ubiquitination Pathway" was also modulated by the up-regulation of UCHL1 and PSMA6 and down-regulation of USP14 and PSMB1. The pathways, "Germ Cell-Sertoli Cell Junction Signaling", "Sertoli Cell-Sertoli Cell Junction Signaling" and "Actin Cytoskeleton Signaling" were modulated by the down-regulation of ACTB, ACTN4, ACTG1 and ACTN1. In addition, "Germ Cell-Sertoli Cell Junction Signaling" and "Sertoli Cell-Sertoli Cell Junction Signaling" pathways were also associated with the down-regulation of CLINT1 and PLS1. Conversely, "Actin Cytoskeleton Signaling" was modulated by the induced expression of PFN1 and CFL1 while "Germ Cell-Sertoli Cell Junction Signaling" was modulated by the up-regulation of CFL1 expression (Table 3).

4. Discussion

In this study, PC-3 and DU145 cells were used as a model of androgen-independent human prostate cancer cells. PC-3 and DU145 cells were metastatic that harbour wild-type and mutant p53, respectively. Despite the biological differences, we identified mutually regulated DEPs as common targets in both cell lines and DEPs mapped to relevant cellular pathways, and their role in anticancer activity was discussed.

ACTB and ACTG associated with structural molecule activity are both actin cytoplasmic proteins implicated in the actin cytoskeletal network that are associated with cell motility and maintenance of the cytoskeleton[10]. Over-expression of ACTG in non-small cell lung cancer cells significantly enhanced cancer cell migration[11] while its down-regulation in neuroblastoma cells resulted in decreased cancer cell migration and motility[12]. Increased expression of ACTB was detected in numerous cancers and was correlated with tumour growth and metastasis[13]. The repressed expression of the two alpha-actinin proteins (ACTN1 and ACTN4) involved in cell migration was also observed in PC-3 and DU145 cells. Alpha-actinins are ubiquitously expressed cytoskeletal proteins that are associated with cytoskeletal integrity and regulation of cell movement. Over-expression of ACTN4 in colorectal cancer cells induced lymph node metastasis in immune-deficient mice while its down-regulation suppressed migration and invasion of cancer cells[14]. Increased ACTN1 expression detected in prostate cancer cells was associated with resistance to zoledronic acid treatment and cancer cells invasion while its decreased expression abolished their resistance to zoledronic acid and inhibited epithelial to mesenchymal transition, reduced focal adhesion kinase and metalloproteases expressions in the cancer cells[15]. The data suggests that the down-regulation of these proteins may have functional roles that impair the tumorigenic responses in the treated prostate cancer cells, thus supporting the anti-cancer role of MS17.

CH60 encoded by *HSPD1* gene, is a highly conserved molecular chaperone found mainly in the mitochondria and some in the cytosol. Interestingly, the expression of CH60 was up-regulated in PC-3 cells while repressed in DU145 cells. It has a dual behaviour, acting either as a tumour suppressor or oncogene depending on the tumour microenvironment. Low level of CH60 expression detected in bladder cancer cells correlated with high tumour stage and was associated with the risk of developing an infiltrating recurrence[16]. Elevated expression of CH60 in gastric cancer was associated with lymph node metastasis, increased cell invasion and poor patient prognosis[17]. In addition, HS71A associated with the similar category also demonstrated opposing regulation in the prostate cancer cells. The expression of HS71A was observed to be repressed in PC-3 cells while up-regulated in DU145 cells.

HS71A belongs to the family of heat shock proteins that functions as ATP-dependent molecular chaperone which supports the folding of newly synthesized polypeptides, transport of protein across cellular membrane and targeting of proteins for lysosomal degradation[18]. Inhibition of this protein stimulates a profound apoptotic response through caspase-3 activation in cancer cells[19]. In contrast, over-expression of HS71A protein expression was also reported to act as cellular chaperone that modulates apoptotic cell death pathways[20,21]. It may be inferred that the induction of the abovementioned protein expressions reflects a similar mechanism by which the exposure of MS17 in the cancer cells induces stress response that may trigger apoptotic activation and impair tumour metastasis in the treated cells.

The mutual down-regulation of HNRPK, PLST and TERA respectively associated with apoptosis, morphogenesis and proteolysis was also noted in both the prostate cancer cells. HNRPK is a RNA binding protein that binds to DNA and RNA in a sequence specific manner, regulates transcription and mRNA metabolism. Up-regulation of HNRPK was associated with cellular migration of cancer cells leading to metastasis while down-regulation of this protein caused decreased migratory activity of the cancer cells[22]. PLST from the family of Plastins is a conserved, versatile modulator of the actin cytoskeleton, which is an important protein in cell migration, adhesion and endocytosis. Increased expression of PLST in colorectal cancer correlated with cancer cell metastasis[23]. Conversely, up-regulation of TERA in colorectal carcinoma repressed apoptosis and sensitivity to chemotherapeutic treatment as well as increased cancer metastasis while its down-regulation inhibited proliferation and invasion, reduced chemoresistance, induced apoptosis and suppressed carcinogenesis *in vivo*[24]. The inhibition of the abovementioned protein expressions by MS17 may similarly modulate its anti-tumorigenic activity in the treated prostate cancer cells.

In the present study, several DEPs modulated by MS17 treated PC-3 and DU145 cells were identified and mapped to relevant biological canonical pathways. In addition to the common proteins, DEPs associated with pathways that were exclusively noted in either PC-3 or DU145 cells were discussed. The top 5 canonical pathways that were significantly activated in PC-3 were associated with cell-cell adhesion and cytoskeletal organization. Notably, the pathways "Remodeling of Epithelial Adherens Junctions", "Epithelial Adherens Junction Signaling", "Sertoli Cell-Sertoli Cell Junction Signaling" and "Germ Cell-Sertoli Cell Junction Signaling" were modulated by the down-regulation of TUBB4B, VCL, ACTB, ACTG1, ACTN4 and ACTN1 while "Paxillin Signaling" was modulated by the down-regulation of VCL, ACTB, ACTG1, ACTN4 and ACTN1. TUBB4B and VCL down-regulation in cancer cells coincides with enhanced drug sensitivity to Eribulin[25] and suppressed cancer cell invasion[26–28] respectively. Similarly, the down-regulation of ACTN1 and ACTN4 expressions has demonstrated involvement in the disruption of cancer progression via induction of anti-metastatic activity and reduced chemotherapy drug resistance[14,15]. Meanwhile, ACTB and ACTG1 are both implicated in the cytoskeletal network. Over-expression of ACTB and ACTG1 in cancer cells was correlated with tumour growth, increased cancer cell migration and metastasis[11,13] while its down-regulation impaired cell migration and motility[12]. The modulation of the abovementioned pathways suggests that MS17 regulates the expression of the cytoskeletal proteins to mediate anti-metastatic, anti-proliferative and anti-invasive activities as well as increase sensitivity to drug treatment in treated PC-3 cells.

Likewise, the modulation of the top five canonical pathways in DU145 cells demonstrated the activation of pathways associated with proteasomal degradation, regulation of electrolytes and water, regulation control of germ cells and organization of filament assembly/disassembly. The pathways, "Protein Ubiquitination Pathway" and "Aldosterone Signaling in Epithelial Cells" were modulated by the induced expressions of HSPA1A/1B, HSP90AA1, HSP90AB1 and HSPB1 and repressed expression of HSPA8, HSPA9 and HSPD1. HSPA1A/1B up-regulation in osteosarcoma cells enhanced drug sensitivity to mitomycin C treatment[29]. While heat shock proteins act as protein chaperones in cellular processes, HSP90AB1 and HSP90AA1 which encode for Hsp90B and Hsp90A respectively are commonly induced during hypoxia which promotes tissue repair mechanism. Hsp90B functions to stabilise the low density lipoprotein receptor-related protein-1 receptor at the cell surface while Hsp90A protein is released into the extracellular space and signals to induce cell migration leading to wound closure[30]. As impaired responses to hypoxia is correlated with cancer progression, this may therefore reflect a similar mechanism by which MS17 up-regulates HSP90AB1 and HSP90AA1 expressions to modulate tissue repair mechanism in treated cells thus contributing to anti-tumorigenesis. Conversely, down-regulation of HSPB1 *in vivo* model of lung carcinoma induced endothelial-to-mesenchymal transition, promoting cancer while[31] its up-regulation inhibited endothelial-to-mesenchymal transition leading to suppressed lung tumorigenesis[32]. Furthermore, these pathways were also modulated by the down-regulation of HSPA8, HSPA9 and HSPD1 protein expressions. Increased HSPA8 expression is commonly associated with tumorigenesis while its inhibition confers anti-proliferative, anti-metastatic and pro-apoptotic properties in endometrial carcinoma cells[33]. Meanwhile, HSPA9 contributes to cell proliferation upon up-regulation but promoted apoptosis and growth arrest following its down-regulation in medullary thyroid carcinoma cells[34]. HSPD1 encodes for CH60 is essential for cell physiology and survival. Up-regulation of CH60 protein in gastric cancer cells was correlated with tumour aggressiveness and poor prognosis[17]. In addition to these proteins, "Protein Ubiquitination Pathway" was also modulated by the up-regulation of UCHL1 and PSMA6 and down-regulation of USP14 and PSMB1 expressions. UCHL1 expression mediates tumour suppressive function and its up-regulation inhibited cell proliferation and demonstrated apoptotic activity in several cancer cells including prostate cancer[35–37]. USP14, a proteasomal deubiquitinating enzyme, was reported to exhibit oncogenic functions in tumour cells upon its induction while its down-regulation suppressed tumour cell proliferation, invasion and promoted apoptosis[38–40]. Induced PSMA6 expression in prostate cancer cells correlated with chemotherapy sensitivity[41] while PSMB1 down-regulation in colorectal cancer cells upon treatment with anticancer agent was associated with apoptotic induction[42]. Hence, the modulation of UCHL1, USP14, PSMB1 and PSMA6 in association with "Protein Ubiquitination Pathway" and "Aldosterone Signaling in Epithelial Cells" pathways may similarly be regulated by MS17 to exhibit apoptotic and anti-proliferative effects observed in the treated cells.

Meanwhile, the pathways "Germ Cell-Sertoli Cell Junction Signaling" and "Sertoli Cell-Sertoli Cell Junction Signaling" were

modulated by the repressed expressions of ACTB, ACTG1, ACTN4 and ACTN1 which were also noted in PC-3 cells. In addition, "Germ Cell-Sertoli Cell Junction Signaling" and "Sertoli Cell-Sertoli Cell Junction Signaling" pathways were also modulated by repressed expressions of CLINT1 and PLS1, which were not identified in PC-3 cells. While literature regarding the anti-cancer role of CLINT1 is limited, the expression of CLINT1 was identified in human osteosarcoma cells and was postulated to be related to cancer cell proliferation[43]. Plastin-1 encoded by PLS1 is an actin-bundling protein which is important to determine architecture of the actin cytoskeleton[44]. Inhibition of PLS1 expression in prostate cancer cells led to reduction of tumour growth and metastasis[45]. Meanwhile, induced expression of CFL1 which encodes for Cofilin-1 was also mapped to the "Germ Cell-Sertoli Cell Junction Signaling" pathway. CFL1 was shown to suppress non-small cell lung cancer cell motility and invasion while selective inhibition of CFL1 conferred cancer cell growth and invasion[46]. Interestingly, activation of "Actin Cytoskeleton Signaling" was also modulated by induced expression of CFL1 and PFN1. PFN1 is a tumour suppressor protein that binds to proline-rich ligands to perform cellular processes such as actin assembly, endocytosis and gene transcription[47]. Over-expression of PFN1 in cancer cells suppressed cell proliferation, motility and invasion resulting in a non-tumorigenic phenotype[48,49]. Taken together, the evidence suggests that the interaction of these proteins in association with the pathways inhibits cell growth via deactivation of proliferative responses and potentially underlies the anti-proliferative and apoptotic activity in MS17 treated DU145 cells.

PC-3 and DU145 are androgen-independent prostate cancer cells with different biological properties, and we identified several mutually regulated proteins by MS17 which could be potential therapeutic targets for these cells. These commonly regulated proteins may inhibit cell proliferation, migration, metastases and induce apoptosis in prostate cancer cells. The pathway analysis revealed genes mapped to the relevant biological pathways were mainly associated with anti-proliferative, anti-metastatic activity and/or apoptosis when treated with MS17. Thus the findings of the current study provide an insight into the antitumor activity of MS17 as a potential chemotherapeutic agent for androgen-independent prostate cancer.

Conflict of interest statement

All the authors declare no conflict of interest.

Acknowledgments

The first author would like to acknowledge the support from the Ministry of Higher Education Malaysia for providing scholarship under the MyBrain (MyPhD) scheme.

Funding

This study was financially supported by the Fundamental Research Grant Scheme, (FRGS/1/2016/SKK08/MUSM/02/1) under the Ministry of Higher Education (MOHE), Malaysia.

References

[1] Huang MT, Lou YR, Xie JG, Ma W, Lu YP, Yen P, et al. Effect of dietary curcumin and dibenzoylmethane on formation of 7,12-dimethylbenz[a] anthracene-induced mammary tumors and lymphomas/leukemias in Sencar mice. *Carcinogenesis* 1998; **19**(9): 1697-1700.

[2] Singh S, Aggarwal BB. Activation of transcription factor NF-kappa B is suppressed by curcumin (diferuloylmethane). *J Biol Chem* 1995; **270**(42): 24995-25000.

[3] Ohori H, Yamakoshi H, Tomizawa M, Shibuya M, Kakudo Y, Takahashi A, et al. Synthesis and biological analysis of new curcumin analogues bearing an enhanced potential for the medicinal treatment of cancer. *Mol Cancer Ther* 2006; **5**(10): 2563-2571.

[4] Adams BK, Cai J, Armstrong J, Herold M, Lu YJ, Sun A, et al. EF24, a novel synthetic curcumin analog, induces apoptosis in cancer cells via a redox-dependent mechanism. *Anticancer Drugs* 2005; **16**(3): 263-275.

[5] Fajardo AM, MacKenzie DA, Ji M, Deck LM, Vander Jagt DL, Thompson TA, et al. The curcumin analog ca27 down-regulates androgen receptor through an oxidative stress mediated mechanism in human prostate cancer cells. *Prostate* 2012; **72**(6): 612-625.

[6] Luo C, Li Y, Zhou B, Yang L, Li H, Feng Z, et al. A monocarbonyl analogue of curcumin, 1,5-bis(3-hydroxyphenyl)-1,4-pentadiene-3-one (Ca 37), exhibits potent growth suppressive activity and enhances the inhibitory effect of curcumin on human prostate cancer cells. *Apoptosis* 2014; **19**(3): 542-553.

[7] Citalingam K, Abas F, Lajis NH, Othman I, Naidu R. Anti-proliferative effect and induction of apoptosis in androgen-independent human prostate cancer cells by 1,5-bis(2-hydroxyphenyl)-1,4-pentadiene-3-one. *Molecules* 2015; **20**(2): 3406-3430.

[8] Paulraj F, Abas F, Lajis NH, Othman I, Hassan SS, Naidu R. The curcumin analogue 1,5-Bis(2-hydroxyphenyl)-1,4-pentadiene-3-one induces apoptosis and downregulates E6 and E7 oncogene expression in HPV16 and HPV18-infected cervical cancer cells. *Molecules* 2015; **20**(7): 11830-11860.

[9] Lee KH, Ab Aziz FH, Syahida A, Abas F, Shaari K, Israf DA, et al. Synthesis and biological evaluation of curcumin-like diarylpentanoid analogues for anti-inflammatory, antioxidant and anti-tyrosinase activities. *Eur J Med Chem* 2009; **44**(8): 3195-3200.

[10]Herman IM. Actin isoforms. *Curr Opin Cell Biol* 1993; **5**(1): 48-55.

[11]Luo Y, Kong F, Wang Z, Chen D, Liu Q, Wang T, et al. Loss of ASAP3 destabilizes cytoskeletal protein ACTG1 to suppress cancer cell migration. *Mol Med Rep* 2014; **9**(2): 387-394.

[12]Shum MS, Pasquier E, Po'uha ST, O'Neill GM, Chaponnier C, Gunning PW, et al. γ-Actin regulates cell migration and modulates the ROCK signaling pathway. *FASEB J* 2011; **25**(12): 4423-4433.

[13]Guo C, Liu S, Wang J, Sun MZ, Greenaway FT. ACTB in cancer. *Clin Chim Acta* 2013; **417**: 39-44.

[14]Honda K, Yamada T, Hayashida Y, Idogawa M, Sato S, Hasegawa F, et al. Actinin-4 increases cell motility and promotes lymph node metastasis of colorectal cancer. *Gastroenterology* 2005; **128**(1): 51-62.

[15]Bizzarro V, Belvedere R, Milone MR, Pucci B, Lombardi R, Bruzzese F, et al. Annexin A1 is involved in the acquisition and maintenance of a stem cell-like/aggressive phenotype in prostate cancer cells with acquired resistance to zoledronic acid. *Oncotarget* 2015; **6**(28): 25076-25092.

[16]Lebret T, Watson RW, Molinie V, O'Neill A, Gabriel C, Fitzpatrick JM, et

al. Heat shock proteins HSP27, HSP60, HSP70, and HSP90: Expression in bladder carcinoma. *Cancer* 2003; **98**(5): 970-977.

[17]Li XS, Xu Q, Fu XY, Luo WS. Heat shock protein 60 overexpression is associated with the progression and prognosis in gastric cancer. *PLoS One* 2014; **9**(9): e107507.

[18]Rohde M, Daugaard M, Jensen MH, Helin K, Nylandsted J, Jaattela M. Members of the heat-shock protein 70 family promote cancer cell growth by distinct mechanisms. *Genes Dev* 2005; **19**(5): 570-582.

[19]Lanneau D, Brunet M, Frisan E, Solary E, Fontenay M, Garrido C. Heat shock proteins: Essential proteins for apoptosis regulation. *J Cell Mol Med* 2008; **12**(3): 743-761.

[20]Parcellier A, Gurbuxani S, Schmitt E, Solary E, Garrido C. Heat shock proteins, cellular chaperones that modulate mitochondrial cell death pathways. *Biochem Biophys Res Commun* 2003; **304**(3): 505-512.

[21]Kennedy D, Jager R, Mosser DD, Samali A. Regulation of apoptosis by heat shock proteins. *IUBMB Life* 2014; **66**(5): 327-338.

[22]Strozynski J, Heim J, Bunbanjerdsuk S, Wiesmann N, Zografidou L, Becker SK, et al. Proteomic identification of the heterogeneous nuclear ribonucleoprotein K as irradiation responsive protein related to migration. *J Proteomics* 2015; **113**: 154-161.

[23]Yokobori T, Iinuma H, Shimamura T, Imoto S, Sugimachi K, Ishii H, et al. Plastin3 is a novel marker for circulating tumor cells undergoing the epithelial-mesenchymal transition and is associated with colorectal cancer prognosis. *Cancer Res* 2013; **73**(7): 2059-2069.

[24]Fu Q, Jiang Y, Zhang D, Liu X, Guo J, Zhao J. Valosin-containing protein (VCP) promotes the growth, invasion, and metastasis of colorectal cancer through activation of STAT3 signaling. *Mol Cell Biochem* 2016; **418**: 189-198.

[25]Dezso Z, Oestreicher J, Weaver A, Santiago S, Agoulnik S, Chow J, et al. Gene expression profiling reveals epithelial mesenchymal transition (EMT) genes can selectively differentiate eribulin sensitive breast cancer cells. *PLoS One* 2014; **9**(8): e106131.

[26]Toma-Jonik A, Widlak W, Korfanty J, Cichon T, Smolarczyk R, Gogler-Piglowska A, et al. Active heat shock transcription factor 1 supports migration of the melanoma cells via vinculin down-regulation. *Cell Signal* 2015; **27**(2): 394-401.

[27]Yoshimoto T, Takino T, Li Z, Domoto T, Sato H. Vinculin negatively regulates transcription of MT1-MMP through MEK/ERK pathway. *Biochem Biophys Res Commun* 2014; **455**(3-4): 251-255.

[28]Li T, Guo H, Song Y, Zhao X, Shi Y, Lu Y, et al. Loss of vinculin and membrane-bound β-catenin promotes metastasis and predicts poor prognosis in colorectal cancer. *Mol Cancer* 2014; **13**: 263.

[29]Nakatsu N, Yoshida Y, Yamazaki K, Nakamura T, Dan S, Fukui Y, et al. Chemosensitivity profile of cancer cell lines and identification of genes determining chemosensitivity by an integrated bioinformatical approach using cDNA arrays. *Mol Cancer Ther* 2005; **4**(3): 399-412.

[30]Jayaprakash P, Dong H, Zou M, Bhatia A, O'Brien K, Chen M, et al. Hsp90 α and Hsp90 β together operate a hypoxia and nutrient paucity stress-response mechanism during wound healing. *J Cell Sci* 2015; **128**(8): 1475-1480.

[31]Potenta S, Zeisberg E, Kalluri R. The role of endothelial-to-mesenchymal transition in cancer progression. *Br J Cancer* 2008; **99**(9): 1375-1379.

[32]Choi SH, Nam JK, Kim BY, Jang J, Jin YB, Lee HJ, et al. HSPB1 inhibits the endothelial-to-mesenchymal transition to suppress pulmonary fibrosis and lung tumorigenesis. *Cancer Res* 2016; **76**(5): 1019-1030.

[33]Shan N, Zhou W, Zhang S, Zhang Y. Identification of HSPA8 as a candidate biomarker for endometrial carcinoma by using iTRAQ-based proteomic analysis. *Onco Targets Ther* 2016; **9**: 2169-2179.

[34]Starenki D, Hong SK, Lloyd RV, Park JI. Mortalin (GRP75/HSPA9) upregulation promotes survival and proliferation of medullary thyroid carcinoma cells. *Oncogene* 2015; **34**(35): 4624-4634.

[35]Ummanni R, Jost E, Braig M, Lohmann F, Mundt F, Barett C, et al. Ubiquitin carboxyl-terminal hydrolase 1 (UCHL1) is a potential tumour suppressor in prostate cancer and is frequently silenced by promoter methylation. *Mol Cancer* 2011; **10**: 129.

[36]Jin C, Yu W, Lou X, Zhou F, Han X, Zhao N, et al. UCHL1 is a putative tumor suppressor in ovarian cancer cells and contributes to cisplatin resistance. *J Cancer* 2013; **4**(8): 662-670.

[37]Xiang T, Li L, Yin X, Yuan C, Tan C, Su X, et al. The ubiquitin peptidase UCHL1 induces G_0/G_1 cell cycle arrest and apoptosis through stabilizing p53 and is frequently silenced in breast cancer. *PLoS One* 2012; **7**(1): e29783.

[38]Zhu Y, Zhang C, Gu C, Li Q, Wu N. Function of deubiquitinating enzyme USP14 as oncogene in different types of cancer. *Cell Physiol Biochem* 2016; **38**(3): 993-1002.

[39]Vogel RI, Pulver T, Heilmann W, Mooneyham A, Mullany S, Zhao X, et al. USP14 is a predictor of recurrence in endometrial cancer and a molecular target for endometrial cancer treatment. *Oncotarget* 2016; **7**(21): 30962-30976.

[40]Zhu L, Yang S, He S, Qiang F, Cai J, Liu R, et al. Downregulation of ubiquitin-specific protease 14 (USP14) inhibits breast cancer cell proliferation and metastasis, but promotes apoptosis. *J Mol Histol* 2016; **47**(1): 69-80.

[41]Milone MR, Pucci B, Bifulco K, Iannelli F, Lombardi R, Ciardiello C, et al. Proteomic analysis of zoledronic-acid resistant prostate cancer cells unveils novel pathways characterizing an invasive phenotype. *Oncotarget* 2015; **6**(7): 5324-5341.

[42]He YJ, Li WL, Liu BH, Dong H, Mou ZR, Wu YZ. Identification of differential proteins in colorectal cancer cells treated with caffeic acid phenethyl ester. *World J Gastroenterol* 2014; **20**(33): 11840-11849.

[43]Ajiro M, Jia R, Yang Y, Zhu J, Zheng ZM. A genome landscape of SRSF3-regulated splicing events and gene expression in human osteosarcoma U2OS cells. *Nucleic Acids Res* 2016; **44**(4): 1854-1870.

[44]Li N, Wong CKC, Cheng CY. Plastins regulate ectoplasmic specialization via its actin bundling activity on microfilaments in the rat testis. *Asian J Androl* 2016; **18**(5): 716-722.

[45]Riplinger SM, Wabnitz GH, Kirchgessner H, Jahraus B, Lasitschka F, Schulte B, et al. Metastasis of prostate cancer and melanoma cells in a preclinical *in vivo* mouse model is enhanced by L-plastin expression and phosphorylation. *Mol Cancer* 2014; **13**: 10.

[46]Tsai CH, Lin LT, Wang CY, Chiu YW, Chou YT, Chiu SJ, et al. Over-expression of cofilin-1 suppressed growth and invasion of cancer cells is associated with up-regulation of let-7 microRNA. *Biochim Biophys Acta* 2015; **1852**(5): 851-861.

[47]Wittenmayer N, Jandrig B, Rothkegel M, Schluter K, Arnold W, Haensch W, et al. Tumor suppressor activity of profilin requires a functional actin binding site. *Mol Biol Cell* 2004; **15**(4): 1600-1608.

[48]Coumans JV, Gau D, Poljak A, Wasinger V, Roy P, Moens PD. Profilin-1 overexpression in MDA-MB-231 breast cancer cells is associated with alterations in proteomics biomarkers of cell proliferation, survival, and motility as revealed by global proteomics analyses. *OMICS* 2014; **18**(12): 778-791.

[49]Yao W, Ji S, Qin Y, Yang J, Xu J, Zhang B, et al. Profilin-1 suppresses tumorigenicity in pancreatic cancer through regulation of the SIRT3-HIF1alpha axis. *Mol Cancer* 2014; **13**: 187.